

A shadowing-based inflation scheme for ensemble data assimilation

Thomas Belsky

Department of Mathematics and Statistics, University of Maine, Orono, ME, USA

Lewis Mitchell*

School of Mathematical Sciences, University of Adelaide, Adelaide, South Australia, Australia

Abstract

Artificial ensemble inflation is a common technique in ensemble data assimilation, whereby the ensemble covariance is periodically increased in order to prevent deviation of the ensemble from the observations and possible ensemble collapse. This manuscript introduces a new form of covariance inflation for ensemble data assimilation based upon shadowing ideas from dynamical systems theory. We present results from a low order nonlinear chaotic system that supports using shadowing inflation, demonstrating that shadowing inflation is more robust to parameter tuning than standard multiplicative covariance inflation, outperforming in observation-sparse scenarios and often leading to longer forecast shadowing times.

Keywords: data assimilation, shadowing, covariance inflation, chaotic dynamics, ensemble methods

2010 MSC: 37C50, 62M20, 93E10, 93E11

*Corresponding author. *Telephone:* +61 8 8313 5424 *Facsimile:* +61 8 8313 3696
Email address: lewis.mitchell@adelaide.edu.au (Lewis Mitchell)
URL: <http://maths.adelaide.edu.au/lewis.mitchell> (Lewis Mitchell)

1. Introduction

Ensemble filtering methods are Monte Carlo approximations to the Bayesian update problem of combining a prior probability density function for a system state with a likelihood function for observational data. Such methods are widely used across the geophysical sciences, for improving forecasts in numerical weather and climate prediction [1, 2] as well as in ocean [3, 4] and atmospheric science [5, 6]. A key advantage of using ensemble methods is the approximation of distributions by finite-size ensembles, leading to a massive computational advantage and the ability to represent otherwise inaccessible high-dimensional distributions [7]. The ensemble Kalman filter (EnKF) [8] along with its variants and extensions such as the local ensemble transform Kalman filter (LETKF) [9] are efficient data assimilation methods which have proven highly effective across a range of applications involving both state and parameter estimation [10, 11, 12, 13].

Ensemble approximations come at an important cost: the use of finite-size ensembles generically leads to sampling errors in ensemble-based Kalman filtering techniques, which can manifest in a number of ways. The most common issue related to insufficient ensemble size is error covariance underestimation, whereby analysis ensemble spreads are routinely underestimated [14]. This can lead to filter divergence where the analysis ensemble becomes overconfident in model forecasts and fails to track the true system states or observations, in some cases even leading to numerical instabilities in the forecast model which ultimately catastrophically diverge to machine infinity [15, 16]. A mechanism for such filter divergence is a finite-size ensemble aligning away from a sufficiently strong attractor, which can lead to integrating a stiff dynamical system [17].

One remedy to counter the underestimation of the error covariance and possible filter divergence is to artificially inflate the ensemble covariance. This artificial inflation can be done simply by periodically adding noise or applying a multiplicative factor greater than one to the error covariance [18, 19]. There also exist adaptive and hybrid covariance inflation methods which modify the

error covariance by accounting for various features of the forecast model and ensemble [20, 21, 22, 23]. There also exist hybrid methods avoiding inflation altogether when the analysis strongly dominates the prior [24]. Other methods to prevent filter divergence involve modifying the basic ensemble filtering algorithms through judicious stochastic parameterization [25, 26]. Finite ensemble sizes can also lead to spurious correlations appearing in the error covariance matrices. Such spurious correlations may be ameliorated by spatially localizing the effects of observations [5], and in rare cases even covariance overestimation, particularly in sparse observational grids [27, 28, 29].

Ideally, a forecast will remain close to the true state or observations for as long as possible and not exhibit any form of divergence, catastrophic or otherwise. Mathematical shadowing theory, developed in the context of hyperbolic systems [30, 31], provides rigorous results guaranteeing the existence of true model trajectories which remain close to a given pseudo-trajectory (one which is almost an actual trajectory of the model) for arbitrarily long times. Such theory has been advanced to show that numerical solutions of chaotic systems do indeed approximate true trajectories [32, 33]. Other studies have determined methods of numerical approximation for hyperbolic periodic orbits that shadow actual periodic orbits [34]. Of course, for non-hyperbolic systems it can be proven that no such shadowing trajectory exists (e.g. [35]), in which case the aim becomes to find shadowing trajectories which nonetheless remain close to pseudo-trajectories with only small mismatches [36].

Operationally, finding shadowing trajectories is greatly limited by model error, confounding sources of error from observations, as well as the sparsity of observations. Nonetheless, [37] proposed a simple method, later extended in [38], for inflating ensemble forecasts in a non-hyperbolic chaotic dynamical system. Their method, which only inflates the ensemble in directions in which uncertainty is shrinking, has had success in increasing the shadowing time of a model forecast.

In this article we introduce a new covariance inflation method for ensemble data assimilation which addresses the general problem of filter divergence

using the shadowing-based approach from [37, 38]. Our method aims to judiciously inflate the ensemble only in directions in which the ensemble is growing overconfident, with the intention of keeping the analysis ensemble close to the attractor. This is done through an algorithm that identifies the contracting ensemble directions over the forecast cycle, and then inflates the ensemble only in these contracting directions before performing the DA analysis. We apply our inflation method within the context of the LETKF, and compare it with the standard multiplicative inflation method via numerical twin experiments on a low-dimensional non-hyperbolic nonlinear chaotic system exhibiting dynamics akin to those in the atmosphere. As we will demonstrate through numerical simulations, the proposed approach works well in sparse observational grids and is less sensitive to parameter tuning than standard methods, while maintaining ensemble reliability.

The remainder of this paper is organized as follows: Section 2 describes ensemble data assimilation and covariance inflation, and proposes the shadowing inflation algorithm used to ameliorate issues related to covariance underestimation. Section 3 details the model and setup of our numerical experiments, and Section 4 presents numerical results comparing standard multiplicative inflation to our proposed shadowing inflation method. We conclude with a discussion in Section 5.

2. Ensemble data assimilation

A general ensemble Kalman filter is a Monte Carlo data assimilation technique based on the Kalman filter [39]. The Kalman filter is an algorithm for determining a state estimate using both a model prediction and observational data. An ensemble Kalman filter is particularly useful, because it extends the linear Kalman filter to nonlinear models and is computationally efficient for large state space vectors [9].

To mathematically describe this type of filter, we assume we have some forecast model M that sequentially determines a model state z . The model

advances the previous analysis state to the forecast state z^f , which at time t_j is:

$$z_j^{f(i)} = M \left(z_{j-1}^{a(i)} \right). \quad (1)$$

Thus, M takes the previous analysis state estimate and updates it forward in time. The index i notates a particular ensemble state, where there are k ensemble states:

$$\left\{ z_{j-1}^{a(i)} : i = 1, 2, \dots, k \right\}. \quad (2)$$

Furthermore, there exist spatial observations of the state at time t_j , denoted by the vector y . Typically, the number of observations is much less than the size of the state space $\dim(y) \ll \dim(z)$. In this formulation, it is assumed that there is a linear observation operator H that projects the state space to the observation space:

$$y_j = H z_j + \epsilon_j. \quad (3)$$

The z_j above represents the true state at time t_j and the observational error is assumed to be a Gaussian random variable $\epsilon_j \sim N(0, R_j)$, where R_j is the covariance matrix for the observations. For simplicity, the time-step notation j will be dropped in the forthcoming notation.

The ensemble Kalman filter [8, 40] is a reduced rank filter, where an ensemble of k analysis states from the previous time step $Z^a = \{z_1^a, z_2^a, \dots, z_k^a\}$ is each individually advanced forward by the forecast model to determine the background forecast ensemble $Z^f = \{z_1^f, z_2^f, \dots, z_k^f\}$. Then the background forecast covariance is formulated as:

$$P^f = \frac{1}{k-1} Z^{f'} (Z^{f'})^T, \quad (4)$$

where the i -th column of $Z^{f'}$ is $z_i^f - \bar{z}^f$, with \bar{z}^f indicating the mean $\bar{z}^f = \frac{1}{k} \sum_{i=1}^k z_i^f$. Thus, the background forecast covariance (4) is not invertible since it is of rank $k-1$, so various ensemble Kalman filter methods perform a change of coordinates to determine a Kalman filter update step, where transform methods avoid computing the background forecast covariance altogether. In particular,

the local ensemble transform Kalman filter (LETKF) [9] updates the covariance analysis as:

$$P^a = Z^{f'} \tilde{P}^a \left(Z^{f'} \right)^T, \quad (5)$$

where \tilde{P}^a represents the analysis error covariance in a k dimensional space:

$$\tilde{P}^a = \left[(k-1)I + (HZ^{f'})^T R^{-1} \left(Z^{f'} \right) \right], \quad (6)$$

and updates each ensemble state as:

$$z_i^a = \bar{z}^f + Z^{f'} \tilde{P}^a \left(HZ^{f'} \right)^T R^{-1} \left(y - Hz_i^f \right). \quad (7)$$

In this study, we use the LETKF as our data assimilation method. The LETKF makes use of localization, where a state location is updated by only considering nearby observations. A basic technique for performing localization is to assign some universal localization radius r , and then only update a state location using observations within r units of that location.

2.1. Covariance inflation

A particular issue with ensemble Kalman filters is that ensemble states often tend to the ensemble mean with small uncertainty. This can lead to the problem of ensemble collapse, where the EnKF analysis leads to an overconfident, but incorrect state. In this case, the low rank P^f underestimates the true uncertainty and the analysis does not shadow the truth.

Ensemble covariance inflation is a procedure to avoid underestimating uncertainties and ensemble collapse. These methods artificially inflate uncertainties in the background covariance. As discussed in the introduction, there are a variety of techniques for performing covariance inflation. One common method is multiplicative inflation, where the background forecast covariance is inflated by a multiplicative factor $1 + \delta$ for $\delta > 0$, thus $P^f \rightarrow (1 + \delta) P^f$. A similar technique is additive inflation, which adds noise Υ to the background covariance $P^f \rightarrow P^f + \Upsilon$.

2.2. Shadowing inflation

We present a new type of covariance inflation, based on ideas from [38]. That work examines how long a forecast ensemble shadows a true solution, but the techniques do not involve any observations or data assimilation. As discussed in the introduction, when an ensemble shadows the true solution, this can be described as the spread of the ensemble (cloud of uncertainty) containing the true solution. Typically, one might begin with a well-distributed ensemble of state solutions $Z_0 \in \mathbb{R}^{N \times k}$ made up of k ensemble members. Each ensemble member is propagated forward by the forecast model M , and a singular value decomposition is performed at each evaluation time step t_j :

$$Z_j = U_j S_j V_j^T, \quad (8)$$

where the resulting singular values (the diagonal components of S_j) determine the length of the axes of ensemble spread and the singular vector U_j determines the direction. This leads to the original sphere of uncertainty evolving into an ellipse, with expanding directions of uncertainty stretching the ellipse and collapsing directions of uncertainty shrinking the ellipse, which is well described in [37]. We remark that in reality the SVD provides a linear approximation to the true ellipse of uncertainty created by the nonlinear evolution of the forecast dynamics, however for short forecast intervals this difference should remain small.

In [38], the concept of stalking, an aggressive form of shadowing, is introduced. Under stalking, at each evaluation time step, artificial uncertainty is inserted in the shrinking directions of the ellipse. Their results determined that the stalking methodology often led to ensembles shadowing the truth for a longer forecast period.

We adapt the idea of ensemble stalking for the purpose of ensemble inflation, which we call ‘shadowing inflation.’ At an assimilation time step t , the forecast model has determined the forecasted ensemble background state $Z^f(t) = Z^f \in \mathbb{R}^{N \times k}$. From this forecasted ensemble state, the shadowing inflation scheme performs the following steps:

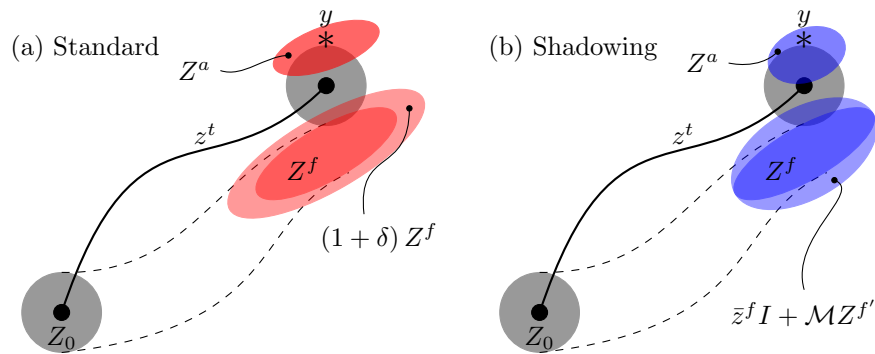


Figure 1: The two figures above are two dimensional cartoons illustrating standard multiplicative inflation and shadowing inflation. In both, there exists an uncertainty for the true trajectory z^t , where the initial data's uncertainty Z_0 is well-distributed about the initial condition. In (a) the forecast model carries forward the ensemble of trajectories to a future time, where some overlap occurs between the actual uncertainty Z^t and the final analysis uncertainty Z^a , after the forecast ensemble Z^f has been inflated by a factor $1 + \delta$ and the observation y has been assimilated. In (b) the proposed shadowing inflation scheme is illustrated, where only the shrinking dimension in the uncertainty Z^f is inflated after the forecast, leading to the analysis ensemble Z^a . The shadowing inflation scheme often leads to a greater overlap between the analysis ensemble and the true uncertainty, with subsequent forecasts achieving a longer shadowing time.

1. Form the matrix: $Z^{f'}(t) = Z^{f'} \in \mathbb{R}^{N \times k}$ (recall the i -th column of $Z^{f'}$ is $z^{f(i)} - \bar{z}^f$) at the beginning of some DA analysis time step t . From a recent, but previous, model step t_- (occurring after the last DA cycle), we also have a forecasted ensemble background state $Z^f(t_-) = Z_-^f$, from which we similarly form: $Z^{f'}(t_-) = Z_-^{f'} \in \mathbb{R}^{N \times k}$. Here, we are implicitly assuming there are multiple forecast steps between each DA cycle. For instance, a numerical weather forecast is typically performed over many incremental time intervals during the 6 hour period between a DA cycle.

2. Perform a singular value decomposition on both: $Z^{f'} = USV^T$ and $Z_-^{f'} = U_-S_-V_-^T$ (here S consists of up to $k - 1$ nonzero singular values $s_i(t)$ and S_- consists of up to $k - 1$ nonzero singular values $s_i(t_-)$). The length and direction of the ensemble ellipsoid (spread) will be determined by $s_i u_i$, where the u_i 's are the columns of U . Due to the non-uniqueness of the SVD, the directions of the singular vectors in U_- need to be matched with their corresponding vectors in U . We do this by calculating the absolute value of the dot products between all pairs of vectors, and then selecting the set of pairs with maximal absolute values.

3. Determine the columns u_c of a new matrix U_c by determining all i for which: $u_c = \{u_i : s_i(t) < s_i(t_-)\}$

4. Form the inflation matrix:

$$\mathcal{M} = I + \delta U_c U_c^T; \quad (9)$$

where $\delta > 0$ is a (small) constant inflation parameter.

5. Finally, form the shadowing inflated background ensemble state: $Z^b(t) = \bar{z}^f I + \mathcal{M} Z^{f'}$, from which the data assimilation process is continued to determine the analysis state.

A schematic diagram illustrating the method plus the analysis step is given in Figure 1. This process only inflates the contracting eigendirections. It performs no inflation on the expanding eigendirections, however this could be easily incorporated (as could a deflation in these directions) if desired, but in the numerical experiments which follow we found that inflating the expanding eigendirections

was detrimental to the analysis.

3. Model and experimental setup

We use the Lorenz-96 model [41] as a test bed for our experiments and results. Lorenz-96 is a conceptual model that determines a ‘weather’ state on a latitude circle:

$$\frac{dz_i}{dt} = (z_{i+1} + z_{i-2})z_{i-1} - z_i + F.$$

In this model, the nonlinear terms mimic advection and conserve the total energy. The linear term dissipates the total energy. F is the forcing, which strongly determines chaotic properties. For our experiments, we take $N = 40$ locations on this latitude circle. We assume the standard forcing $F = 8$, which corresponds to a chaoticity similar to true atmospheric dynamics [41]. The climatological standard deviation for the system with these parameters is $\sigma_{\text{clim}} = 3.63$.

For this model and choice of parameters, a time-step of $h = 0.05$ simulates a 6 hour Earth weather forecast [41]. We discretize this model on a $h/10$ time-step, performing DA updates at multiples of h . When performing shadowing inflation, we determine the expanding (and contracting) directions of uncertainty by examining the singular value decomposition at the assimilation time step t_a and the previous model step $t_a - h/10$.

We run the model for 110 days of model time ($t = 22$), create synthetic observations by adding Gaussian noise with error covariance $R = 0.2I$ to every observed N_{obs} spatial location, and allow the system to spin up for 10 days from an arbitrary initial condition before performing experiments. We perform 100 separate simulations, where our results provide the mean of the RMS error and the corresponding 95% confidence interval. We use $k = 20$ ensemble members in all experiments, and unless specified otherwise we take a constant inflation parameter $\delta = 0.02$ in Equation 9 (which is equivalent to a fixed multiplicative inflation factor of 1.02), localization radius $r = 5$, which we found to produce the best performance in the LETKF with global multiplicative inflation, and set $N_{\text{obs}} = 8$ fixed observations.

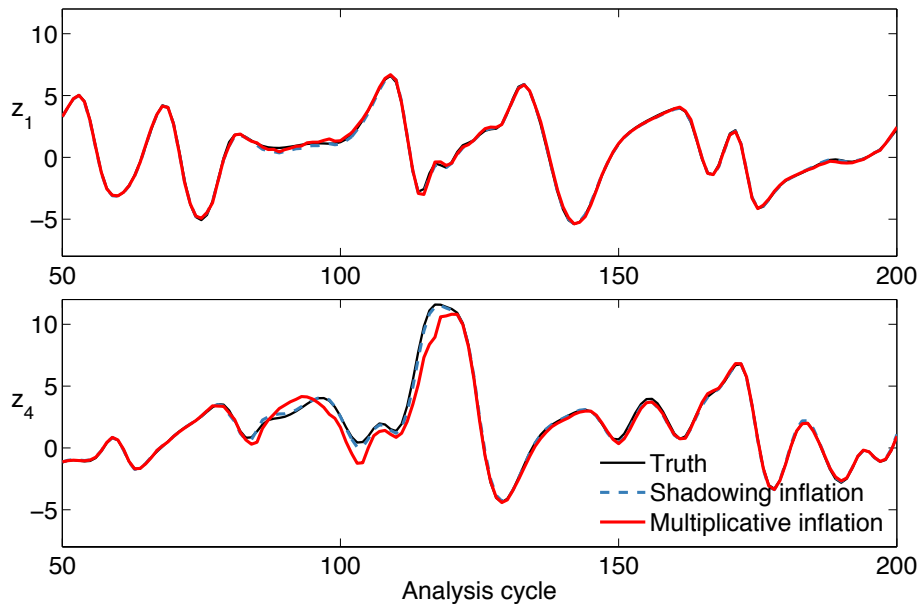


Figure 2: Example analysis trajectories for standard (red, solid) and shadowing (blue, dashed) methods. Top: observed component. Bottom: unobserved component. Black, solid line shows the truth.

4. Results

Firstly, in Figure 2 we show example analyses made by the standard multiplicative inflation and shadowing inflation methods, for an observed and unobserved component of Lorenz-96. While both inflation methods track the observed component equally well, the shadowing inflation tracks the unobserved component of the truth more closely, especially between analysis cycles 85 and 120, where the standard method diverges noticeably from the truth.

We focus more on this improvement shadowing inflation makes over the standard scheme in Figure 3, where we show individual ensemble member trajectories between analysis cycles 120 and 140. Where the true trajectory passes through extrema, the standard inflation scheme greatly overinflates the ensemble, leading to a poor representation of the true trajectory near the turning point. On the other hand, the shadowing inflation scheme avoids this over-

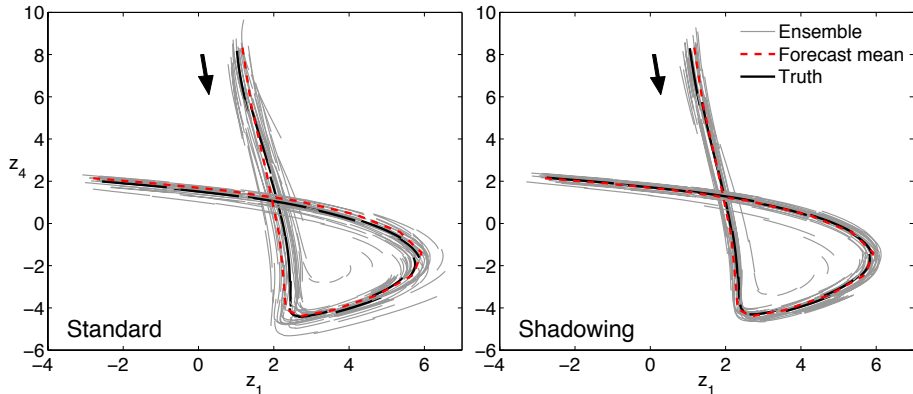


Figure 3: Example ensemble trajectories for standard (left) and shadowing (right) inflation schemes. The grey trajectories show forecasts generated by individual ensemble members after each analysis, while the red dashed line shows the mean of these ensemble forecasts. The solid black line shows the true trajectory being estimated.

inflation by only inflating the ensemble in contracting directions, leading to an ensemble which is more tightly clustered around the truth. This suggests that shadowing inflation is most beneficial near the edges of the model attractor, similar to results in [38] for the forecasting problem. We might also expect shadowing inflation to outperform the standard method near the stable manifold of a saddle, where trajectories in the analysis ensemble might diverge dramatically due to being falsely initialized on both sides of the manifold. Note also that while the analysis mean for each ensemble is not visibly dissimilar in our example (Figure 2, analysis cycles 120–140), there is a substantial difference in how well each ensemble represents the truth. Indeed, in Figure 3 the forecast mean (red dashed line) in this region is reasonably close to the truth and not dissimilar between the two inflation methods, however the ensemble spread is noticeably worse for the global multiplicative inflation.

Figure 2 suggests that the shadowing inflation scheme is most beneficial in the unobserved subspace. To explore this we plot total RMS errors as a function of the number of observations in Figure 4a, as well as the RMS errors in

the unobserved and observed subspaces (Figures 4b and 4c respectively). Both methods diverge from the truth for small numbers of observations, but with the shadowing method diverging less strongly than the multiplicative inflation method. Note that in the observed subspace both methods produce analyses with errors less than the observational noise of standard deviation $\sqrt{0.2} \approx 0.44$, and in the unobserved subspace the RMS errors are no worse than the climatological standard deviation $\sigma_{\text{clim}} = 3.63$. While the shadowing scheme performs worse than the standard scheme in the observed subspace for $5 \leq N_{\text{obs}} \leq 7$, shadowing performs noticeably better than the standard method in the much larger unobserved subspace over the same range of N_{obs} .

To compare the robustness of the shadowing and standard inflation schemes further, Figure 5 explores the sensitivity of the two methods to the choice of inflation parameter δ . This figure varies the shadowing inflation factor δ from 0.005 to 0.1, and equivalently varies the fixed multiplicative inflation factor $1 + \delta$ from 1.005 to 1.1. Figures 5a-c respectively plot the mean and the 95% confidence interval of the RMS error of the multiplicative inflation scheme (solid, red) and the shadowing inflation scheme (dashed, blue) for a) all locations, b) only observed locations, c) only unobserved locations. We see that the shadowing inflation scheme is much more robust to the predetermined inflation factor than the multiplicative scheme, which has a large increase in error for values larger than $\delta = 0.05$. Figure 5d plots the mean of the trace of the analysis covariance P^a over all time steps, effectively showing that the shadowing scheme is again less sensitive to the inflation factor than the multiplicative scheme, which overestimates the analysis uncertainty for larger inflation factors.

Figure 6 plots the RMS error of 10 day forecasts performed after the 110 day DA simulation for both the multiplicative inflation scheme (solid, red) and the shadowing inflation scheme (dashed, blue). Figure 6a is for an inflation factor of $\delta = 0.02$, Figure 6b is for an inflation factor of $\delta = 0.05$, and Figure 6c is for an inflation factor of $\delta = 0.10$. In all three we see that the multiplicative scheme leads to a much smaller spread between realizations than the shadowing scheme, especially at the beginning of each forecast. As illustrated in Figure 3,

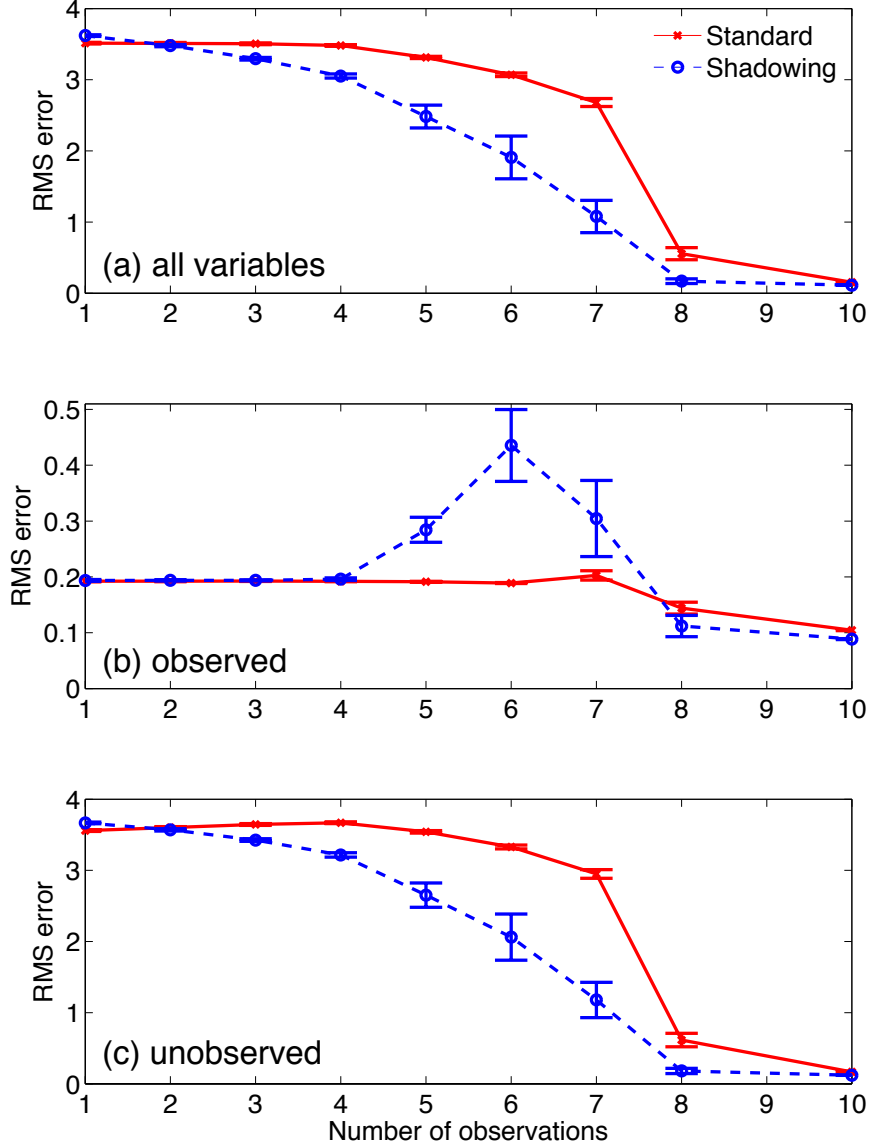


Figure 4: Dependence of RMS errors upon number of observations N_{obs} for multiplicative (red, x) and shadowing (blue, o) inflation schemes. Subplots show errors averaged over (a) all variables; (b) observed variables; (c) unobserved variables. For comparison, the climatological standard deviation is $\sigma_{\text{clim}} = 3.63$ and observational error standard deviation is $\sqrt{0.2} \approx 0.44$.

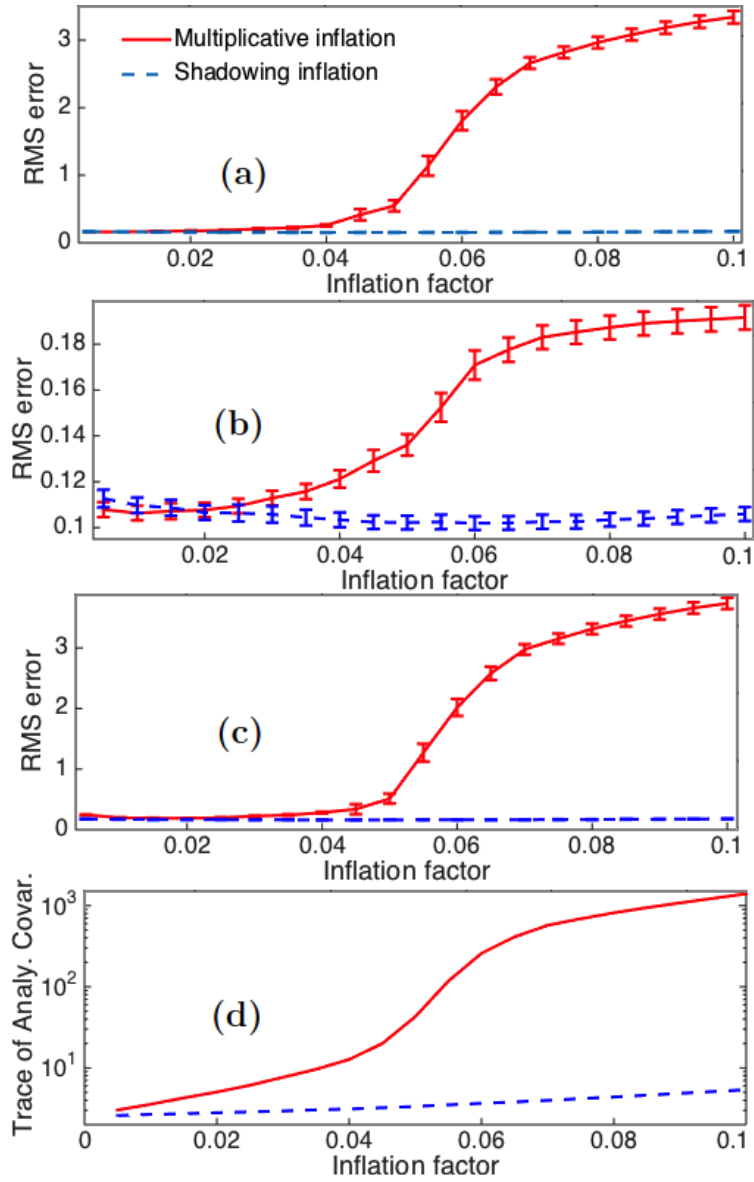


Figure 5: Top three figures above plot the mean and the 95% confidence interval of the RMS error of the multiplicative inflation scheme (solid, red) and the shadowing inflation scheme (dashed, blue), varying the inflation factor. (a) is the RMS error of all locations, (b) is the RMS error of observed locations, and (c) is the RMS error of unobserved locations. (d) plots $tr(P^a)$. Here, the localization radius is $r = 5$ and there are 8 fixed observations.

the shadowing inflation can lead to a better forecast, since it better spreads the ensemble of trajectories about the observed true trajectory. For Figures 6b and Figure 6c the forecasted solution, or shadowing time, of the shadowing inflation scheme substantially outperforms the multiplicative inflation scheme.

Finally, we show that shadowing inflation improves ensemble reliability by comparing ranked probability histograms for the two schemes [42]. Figure 7 shows ranked probability histograms for the shadowing and standard methods. The convex shape of the diagrams indicates that both methods are overdispersive, however the shadowing method is significantly less underconfident (across both observed and unobserved variables) than the standard method is.

5. Discussion

This work has introduced a new shadowing-based inflation method for ensemble data assimilation. We have tested this shadowing inflation scheme numerically on a low-dimensional nonlinear system exhibiting chaotic dynamics reminiscent of those in the atmosphere. Comparing shadowing inflation with standard global multiplicative covariance inflation, we have found that shadowing outperforms the standard method in sparse observational grids, maintains ensemble reliability, often leads to longer forecast shadowing times, and is relatively insensitive to parameter tuning.

All experiments for the present work were performed using a perfect model – an obvious area for further exploration is the case of model error, where ensemble inflation must compensate for structural deficiencies in the forecast model. That shadowing inflation tends to perform best at the extremities of the attractor (as shown in Figure 3) suggests that it might be a useful method in situations involving model error, as it is near these extremes, or near a saddle point in the stable manifold, where model error should have a large detrimental effect. Future work will involve coupling shadowing inflation methods with known methods for dealing with model error [43].

The present work also uses a constant inflation factor, regardless of where in

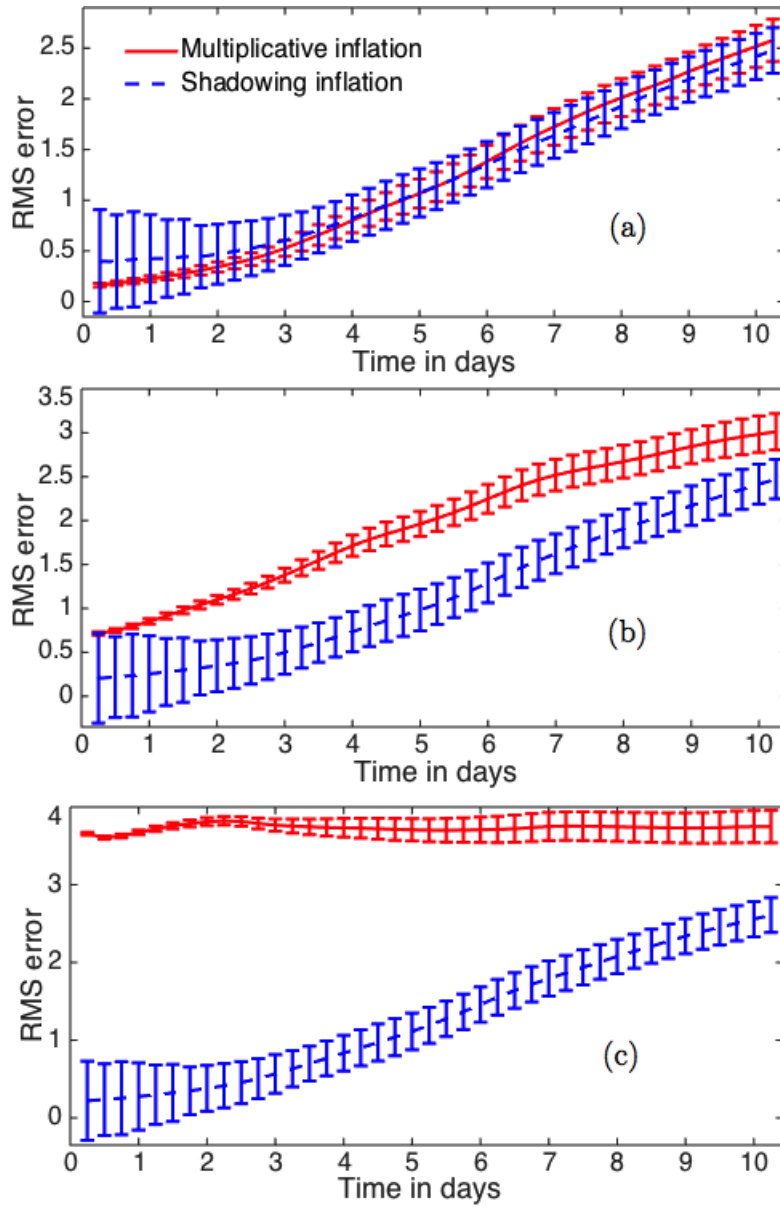


Figure 6: This figure plots the mean and the 95% confidence interval of the RMS error of the multiplicative inflation scheme (solid, red) and the shadowing inflation scheme (dashed, blue) for a ten day forecast at the end of the 110 day DA simulation. (a) is for an inflation factor of $\delta = 0.02$, (b) is for an inflation factor of $\delta = 0.05$, and (c) is for an inflation factor of $\delta = 0.10$. Here, the localization radius is $r = 5$ and there are 8 fixed observations.

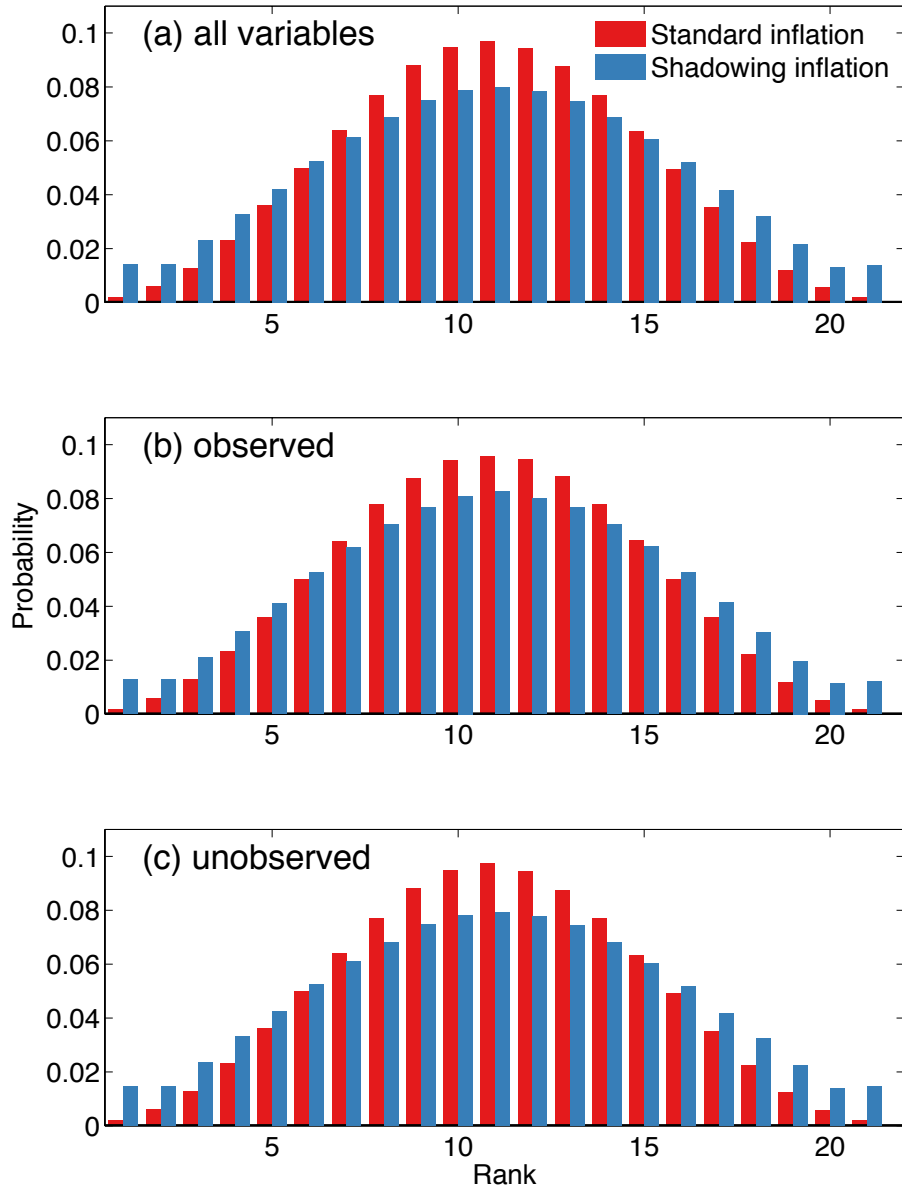


Figure 7: Rank histograms, $N_{obs} = 8$, $r = 5$, $\delta = 0.02$.

state space the inflation is being performed. However, as shown in [38] for the forecasting problem, it can be beneficial to perform adaptive inflation depending on the location of the forecast on the model attractor. While we noticed no significant difference when making the inflation factor dependent on the level of expansion measured by the singular values s_i , a more attractor-based scheme may show further improvements. Note that such methods would necessarily be constrained to low-dimensional systems where the shape of the attractor can be reasonably estimated.

For simplicity we formulated the method here involving an extra SVD of the full forecast ensemble deviation matrix, which would be computationally impractical in large systems. However, significant computational savings could be made by performing the shadowing inflation within the ensemble space, utilizing the SVD step which is already performed as part of the LETKF algorithm. Future work will formulate a shadowing inflation scheme within the ensemble subspace and compare the accuracy and computational cost when making this modification.

Acknowledgments

The authors acknowledge National Science Foundation support DMS-0940271 and DMS-0940314. They also are thankful for support from the Mathematics and Climate Research Network.

References

References

- [1] K. Hayden, E. Olson, E. S. Titi, Discrete data assimilation in the Lorenz and 2d Navier–Stokes equations, *Physica D: Nonlinear Phenomena* 240 (18) (2011) 1416–1425.
- [2] F. Rabier, Overview of global data assimilation developments in numerical weather-prediction centres, *Quarterly Journal of the Royal Meteorological*

Society 131 (613) (2005) 3215–3233. doi:10.1256/qj.05.129.

URL <http://doi.wiley.com/10.1256/qj.05.129>

- [3] G. Evensen, Inverse methods and data assimilation in nonlinear ocean models, *Physica D: Nonlinear Phenomena* 77 (1) (1994) 108–129.
- [4] G. Vernieres, C. K. Jones, K. Ide, Capturing eddy shedding in the Gulf of Mexico from Lagrangian observations, *Physica D: Nonlinear Phenomena* 240 (2) (2011) 166–179. doi:10.1016/j.physd.2010.06.008.
URL <http://linkinghub.elsevier.com/retrieve/pii/S0167278910001855>
- [5] J. L. Anderson, Exploring the need for localization in ensemble data assimilation using a hierarchical ensemble filter, *Physica D: Nonlinear Phenomena* 230 (1) (2007) 99–111.
- [6] E. Kalnay, *Atmospheric Modeling, Data Assimilation, and Predictability*, Cambridge University Press, Cambridge, 2002.
- [7] P. L. Houtekamer, H. L. Mitchell, A sequential ensemble kalman filter for atmospheric data assimilation, *Monthly Weather Review* 129 (1) (2001) 123–137.
- [8] G. Evensen, Sequential data assimilation with a nonlinear quasi-geostrophic model using Monte-Carlo methods to forecast error statistics, *Journal of Geophysical Research* 99 (1994) 10143–10162.
- [9] B. Hunt, E. Kostelich, I. Szunyogh, Efficient data assimilation for spatiotemporal chaos: A local ensemble transform Kalman filter, *Physica D* 230 (2007) 112–126.
- [10] T. DelSole, X. Yang, State and parameter estimation in stochastic dynamical models, *Physica D: Nonlinear Phenomena* 239 (18) (2010) 1781–1788.
- [11] T. Bellsky, E. J. Kostelich, A. Mahalov, Kalman filter data assimilation: Targeting observations and parameter estimation, *Chaos: An Interdisciplinary Journal of Nonlinear Science* 24 (2) (2014) 024406. doi:

10.1063/1.4871916.

URL <http://scitation.aip.org/content/aip/journal/chaos/24/2/10.1063/1.4871916>

- [12] T. Belsky, J. Berwald, L. Mitchell, Nonglobal Parameter Estimation Using Local Ensemble Kalman Filtering, *Monthly Weather Review* 142 (6) (2014) 2150–2164. doi:10.1175/MWR-D-13-00200.1.
URL <http://dx.doi.org/10.1175/MWR-D-13-00200.1>
- [13] M. Kretschmer, B. R. Hunt, E. Ott, Data assimilation using a climatologically augmented local ensemble transform kalman filter, *Tellus A* 67 (2015) 26617.
- [14] H. Li, E. Kalnay, T. Miyoshi, Simultaneous estimation of covariance inflation and observation errors within an ensemble kalman filter, *Quarterly Journal of the Royal Meteorological Society* 135 (639) (2009) 523–533.
- [15] D. Kelly, A. J. Majda, X. T. Tong, Concrete ensemble kalman filters with rigorous catastrophic filter divergence, *Proceedings of the National Academy of Sciences* 112 (34) (2015) 10589–10594.
- [16] J. Harlim, A. J. Majda, Catastrophic filter divergence in filtering nonlinear dissipative systems, *Communications in Mathematical Sciences* 8 (1) (2010) 27–43.
URL <http://projecteuclid.org/euclid.cms/1266935012>
- [17] G. A. Gottwald, A. J. Majda, A mechanism for catastrophic filter divergence in data assimilation for sparse observation networks, *Nonlinear Processes in Geophysics* 20 (5) (2013) 705–712. doi:10.5194/npg-20-705-2013.
URL <http://www.nonlin-processes-geophys.net/20/705/2013/>
- [18] G. Evensen, *Data assimilation: the ensemble Kalman filter*, Springer Science & Business Media, 2009.

- [19] G. Burgers, P. Jan van Leeuwen, G. Evensen, Analysis scheme in the ensemble kalman filter, *Monthly weather review* 126 (6) (1998) 1719–1724.
- [20] H. L. Mitchell, P. Houtekamer, An adaptive ensemble kalman filter, *Monthly Weather Review* 128 (2) (2000) 416–433.
- [21] J. L. Anderson, An adaptive covariance inflation error correction algorithm for ensemble filters, *Tellus A* 59 (2) (2007) 210–224.
- [22] J. L. Anderson, Spatially and temporally varying adaptive covariance inflation for ensemble filters, *Tellus A* 61 (1) (2009) 72–83.
- [23] T. Miyoshi, The gaussian approach to adaptive covariance inflation and its implementation with the local ensemble transform kalman filter, *Monthly Weather Review* 139 (5) (2011) 1519–1535.
- [24] M. Bocquet, P. N. Raanes, A. Hannart, Expanding the validity of the ensemble kalman filter without the intrinsic need for inflation, *Nonlinear Processes in Geophysics* 22 (6) (2015) 645–662.
- [25] J. Harlim, A. J. Majda, Filtering Turbulent Sparsely Observed Geophysical Flows, *Monthly Weather Review* 138 (4) (2010) 1050–1083. doi:10.1175/2009MWR3113.1.
- [26] L. Mitchell, G. A. Gottwald, Data Assimilation in Slow–Fast Systems Using Homogenized Climate Models, *Journal of the Atmospheric Sciences* 69 (4) (2012) 1359–1377. doi:10.1175/JAS-D-11-0145.1.
- [27] J. Liu, E. Fertig, H. Li, E. Kalnay, B. R. Hunt, E. Kostelich, I. Szunyogh, R. Todling, Comparison between Local Ensemble Transform Kalman Filter and PSAS in the NASA finite volume GCM – perfect model experiments, *Nonlinear Processes in Geophysics* 15 (2008) 645–659.
URL <http://arxiv.org/abs/physics/0703066>
- [28] J. S. Whitaker, G. P. Compo, J.-N. Thépaut, A Comparison of Variational and Ensemble-Based Data Assimilation Systems for Reanalysis of Sparse

- Observations, *Monthly Weather Review* 137 (6) (2009) 1991–1999. doi: 10.1175/2008MWR2781.1.
- [29] G. A. Gottwald, L. Mitchell, S. Reich, Controlling Overestimation of Error Covariance in Ensemble Kalman Filters with Sparse Observations: A Variance-Limiting Kalman Filter, *Monthly Weather Review* 139 (8) (2011) 2650–2667. doi:10.1175/2011MWR3557.1.
URL <http://journals.ametsoc.org/doi/abs/10.1175/2011MWR3557.1>
- [30] D. V. Anosov, Geodesic flows on closed riemannian manifolds with negative curvature, *Proc. Steklov Inst. Math.* 90 (1969) 1–235.
URL <http://ci.nii.ac.jp/naid/10006655233/en/>
- [31] R. Bowen, ω -Limit sets for Axiom A diffeomorphisms, *Journal of Differential Equations* 18 (2) (1975) 333–339. doi:10.1016/0022-0396(75)90065-0.
URL <http://www.sciencedirect.com/science/article/pii/0022039675900650>
- [32] S. M. Hammel, J. A. Yorke, C. Grebogi, Do numerical orbits of chaotic dynamical processes represent true orbits?, *Journal of Complexity* 3 (2) (1987) 136–145.
- [33] S. M. Hammel, J. A. Yorke, C. Grebogi, et al., Numerical orbits of chaotic processes represent true orbits, *American Mathematical Society* 19 (2) (1988) 465–469.
- [34] E. S. Van Vleck, Numerical shadowing near hyperbolic trajectories, *SIAM Journal on Scientific Computing* 16 (5) (1995) 1177–1189.
- [35] E. J. Kostelich, I. Kan, C. Grebogi, E. Ott, J. A. Yorke, Unstable dimension variability: A source of nonhyperbolicity in chaotic systems, *Physica D: Nonlinear Phenomena* 109 (1-2) (1997) 81–90. doi:10.1016/S0167-2789(97)00161-9.

- [36] K. Judd, C. A. Reynolds, T. E. Rosmond, L. A. Smith, The Geometry of Model Error, *Journal of the Atmospheric Sciences* 65 (6) (2008) 1749–1772. doi:10.1175/2007JAS2327.1. URL <http://journals.ametsoc.org/doi/abs/10.1175/2007JAS2327.1>
- [37] C. M. Danforth, J. Yorke, Making Forecasts for Chaotic Physical Processes, *Physical Review Letters* 96 (14) (2006) 1–4. doi:10.1103/PhysRevLett.96.144102. URL <http://link.aps.org/doi/10.1103/PhysRevLett.96.144102>
- [38] R. M. Lieb-Lappen, C. M. Danforth, Aggressive shadowing of a low-dimensional model of atmospheric dynamics, *Physica D* 241 (6) (2012) 637–648.
- [39] R. Kalman, A new approach to linear filtering and prediction problems, *Trans. of the ASME J. of Basic Eng.* 82 (1960) 35–45.
- [40] P. L. Houtekamer, H. L. Mitchell, Data assimilation using an ensemble kalman filter technique, *Monthly Weather Review* 126 (3) (1998) 796–811.
- [41] E. N. Lorenz, Predictability: A problem partly solved, in: *Seminar on Predictability*, ECMWF, Reading, 1996, pp. 1–18. URL <http://scholar.google.com/scholar?hl=en&btnG=Search&q=intitle:Predictability:+A+problem+partly+solved#0>
- [42] D. S. Wilks, *Statistical methods in the atmospheric sciences*, Vol. 100, Academic press, 2011.
- [43] L. Mitchell, A. Carrassi, Accounting for model error due to unresolved scales within ensemble kalman filtering, *Quarterly Journal of the Royal Meteorological Society* 141 (689) (2015) 1417–1428. doi:10.1002/qj.2451. URL <http://dx.doi.org/10.1002/qj.2451>